SUPPLEMENTARY DATA

Supplementary Figure 1. Sorcin expression levels in islets of SRI-tg mice. (A-B) Total protein and mRNA were extracted from islets isolated from **(A)** SRI-tg1 and **(B)** SRI-tg10 mice (n=3-6 per genotype, 8-11 weeks old) and their respective littermate controls receiving doxycycline in the drinking water from 4 weeks old. Top panels show representative Western blots performed as in (Leclerc, et al., Am J Physiol Endocrinol Metab, 2004, 286(6):E1023-31) using rabbit polyclonal anti-sorcin (1:1000, Farrell, et al., J Biol Chem, 2003, 278(36):34660-6) and mouse monoclonal anti-alpha tubulin (1:20000, Sigma #T5168). Lower panels show qRT-PCR analysis of sorcin and luciferase expression. Values are mean ± SEM. Statistics: *p<0.05, **p<0.01, ***p<0.001, two-tailed Student's t tests.

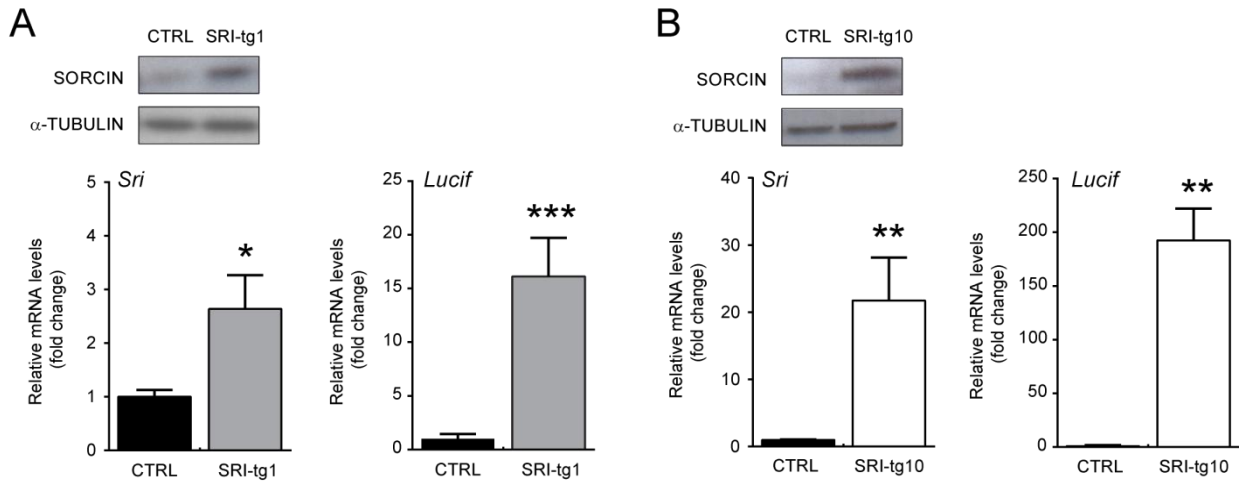

SUPPLEMENTARY DATA

Supplementary Figure 2. Sorcin phenotype is not apparent *in vivo* in the absence of β cell stress. (A, C) IPGTTs in SRI-tg1 male mice under standard chow diet (SD) (*n*=10-12, 16 and 24 weeks old as indicated). **(B, D)** IPGTTs in SRI-tg10 female mice under HFD (*n*=7-11, 16 and 24 weeks old as indicated). SRI-tg10 females, which are more resistant to diet-induced lipotoxicity than males (Oliveira et al., Ann Anat, 2015, 10.1016/j.aanat.2015.01.007), display an improved glucose tolerance only after 20 weeks of HFD. Right panels represent AUC of blood glucose concentration during IPGTTs. Values are mean ± SEM. ***p<0.001; Two-way ANOVA.

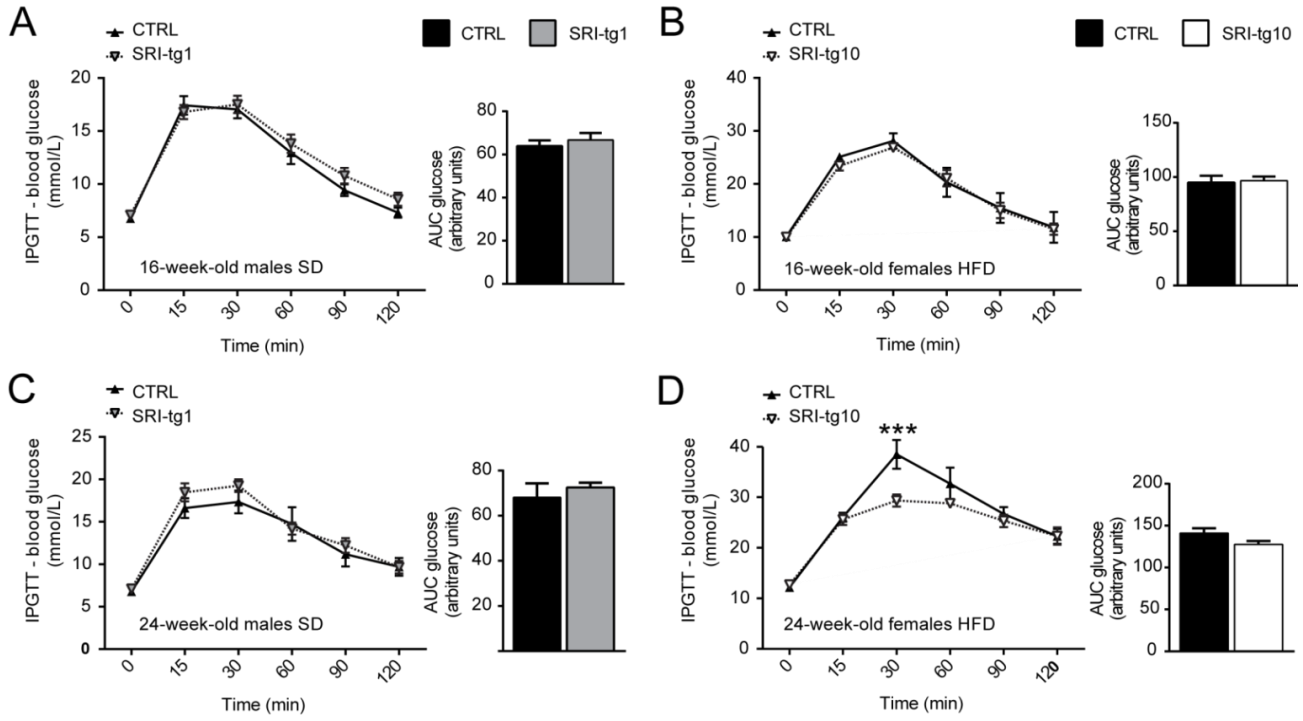

SUPPLEMENTARY DATA

Supplementary Figure 3. Sorcin overexpression enhances GSIS in isolated islets of SRI-tg1 mice. *Ex vivo* insulin secretion assays were performed on isolated islets from HFD-fed SRI-tg1 male mice (*n*=3, 17-week-old). Mice were sacrificed by cervical dislocation and pancreatic islets were isolated by *in situ* collagenase digestion and cultured as previously described (Ravier, et al., Methods Mol Biol, 2010). Transgenic islets were cultured overnight in medium supplemented with 0.5µg/ml doxycycline hyclate to sustain transgene expression. Islets were divided into groups of 10 islets per condition and insulin secretion assays were performed as described in (Leclerc, et al., Am J Physiol Endocrinol Metab, 2004, 286(6):E1023-31). Secreted and total insulin content were quantified using HTRF Insulin kit (Cisbio). *p<0.05, two-tailed Student's t tests.

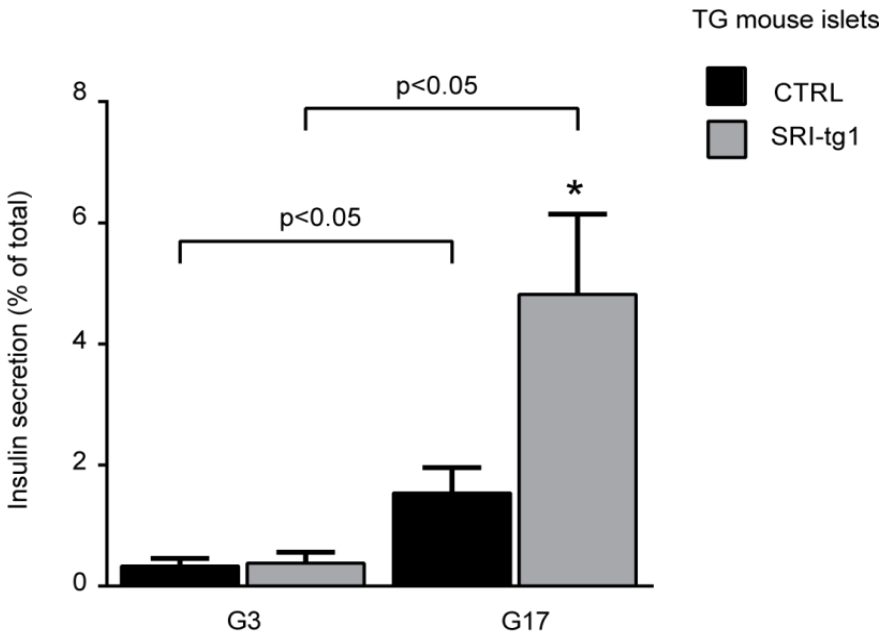

SUPPLEMENTARY DATA

Supplementary Figure 4. Sorcin overexpression in human islets enhances glucose-induced intracellular Ca^{2+} oscillations. Cytosolic free Ca^{2+} levels ($[Ca^{2+}]_{cyt}$) were measured in islets from human cadaveric donors (*n*=3, see Supplemental Table 2 for donors characteristics) transduced with an adenovirus encoding sorcin-GFP or GFP only. Dissociated islets were loaded with Fura-Red (Invitrogen; 4 µM) then perifused sequentially with 3 mM glucose (G3), 17 mM glucose (G17), G17 and KCl (20 mM), and G3 as indicated. Different types of responses for glucose-stimulated $[Ca^{2+}]_{cyt}$ increases were observed and quantified as follows: (i) no response to G17, (ii) low response to G17 (peaks > 0.3 and < 4 % over basal) and (iii) high response to G17 (peaks > 4 % over basal). (**A**) Representative traces of non-responsive (i), low-responsive (ii) and high-responsive (iii) islets. (**B**) Quantification of results. *p<0.05, Two-tailed Student's t-tests.

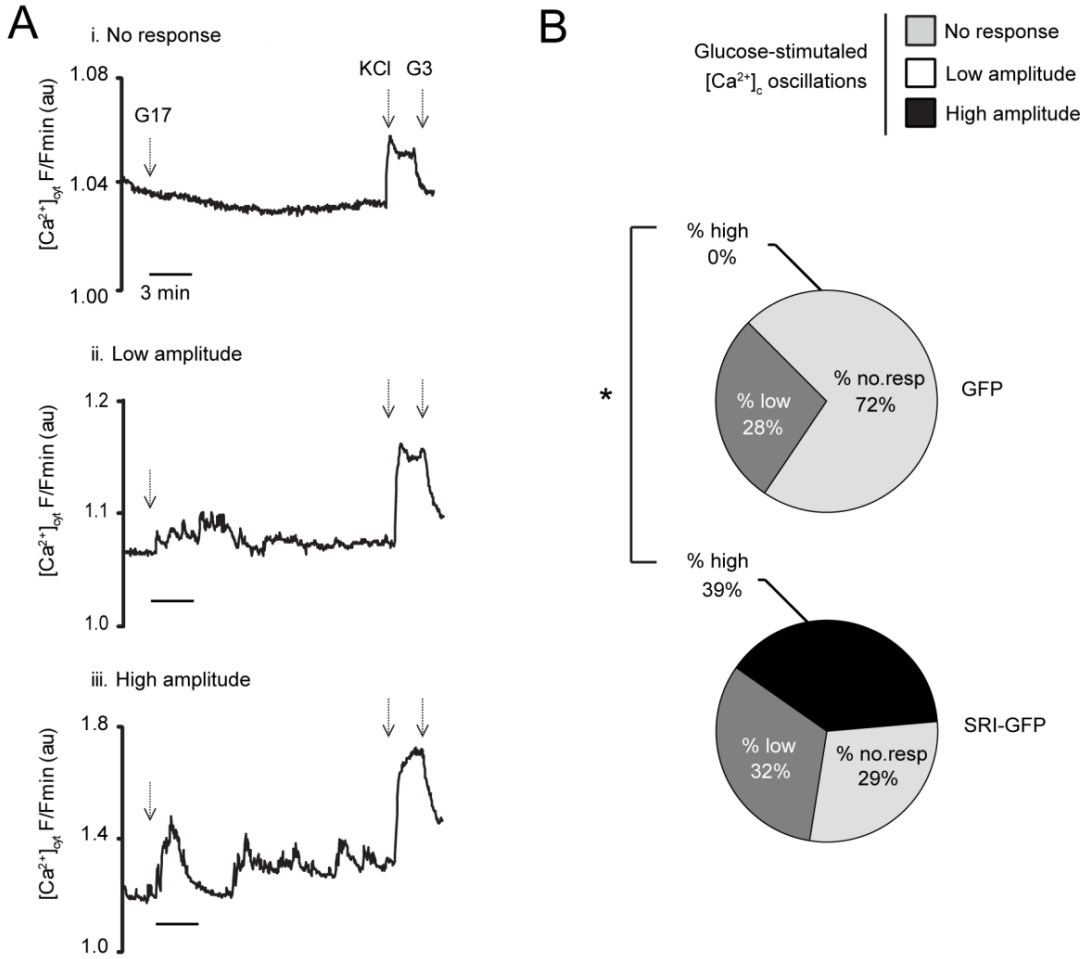

SUPPLEMENTARY DATA

Supplementary Figure 5. Sorcin overexpression no longer enhances glucose-stimulated cytosolic Ca^{2+} levels after ER Ca^{2+} depletion. Cytosolic Ca^{2+} levels ($[Ca^{2+}]_{cyt}$) were measured in intact islets loaded with Fluo-2 MA AM (Cambridge Bioscience) from HFD-fed SRI-tg10 male mice and littermate controls (*n*=4, 11-week-old). The islets were perifused sequentially with 3 mM glucose (G3) in the presence of the SERCA pump inhibitor, cyclopiazonic acid (CPA, 20 µM, Sigma #C1530) to empty the ER, followed by 17 mM glucose (G17) glucose as indicated. Traces represent mean ± SEM. The right panel represents AUC of $[Ca^{2+}]_c$ after glucose stimulation (time: 13-22 min). Two-tailed Student's t-tests.

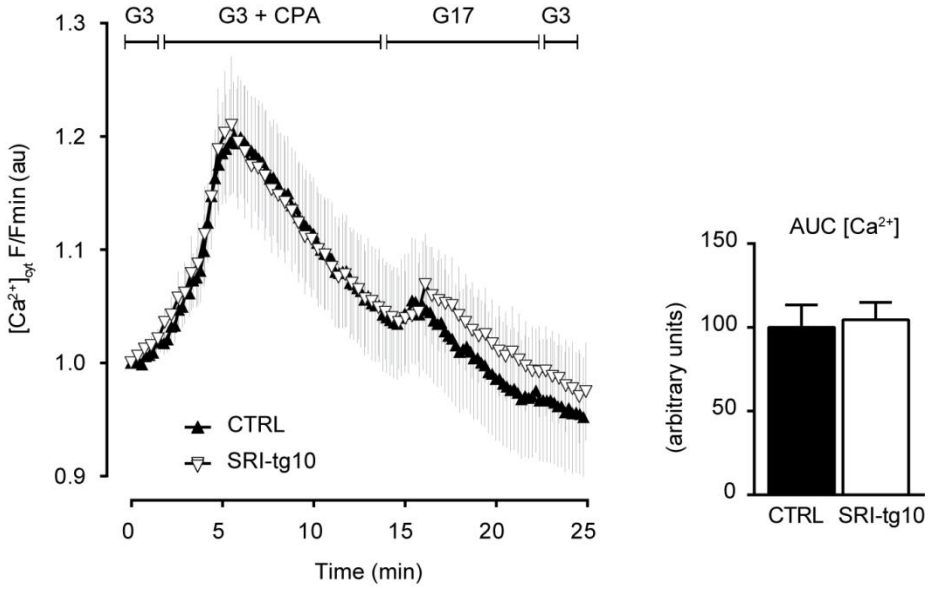

SUPPLEMENTARY DATA

Supplementary Figure 6. Endogenous sorcin expression in regular chow and high fat fed DBA2/J mice. Normalised RNA-Seq counts for Sri compared between regular chow and high fat diet fed mice at 30 days, six biological replicates per condition. To obtain counts, reads were mapped to mm9 and summed for all exons of a gene. The gene counts were then normalised using EdgeR and differential expression measured using a moderated t-test in limma (voom method). P-values were corrected for multiple comparisons using the Benjamini Hochberg FDR method. The estimated fold change and corrected p-value are indicated.

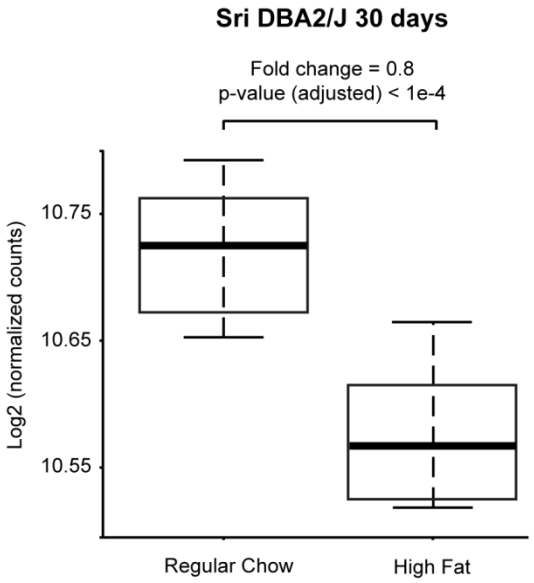

SUPPLEMENTARY DATA

Supplementary Figure 7. Effects of diazoxide and cyclosporine A on hG6PC2 promoter activity. MIN6 β cells were co-transfected with pRL-CMV and -1075+124hG6PC2-Luci using Lipofectamine 2000 and OptiMem. After 20h (overnight) the medium was changed for 20 mM Glucose DMEM supplemented with DMSO (0.1%), diazoxide (Diaz, 100 μM) or cyclosporin A (CsA, 0.2 μM) as indicated for a further 24h before cell lysis and luciferase assays (*n*=3-4 independent experiments). Values are mean ± SEM. **p<0.005, ***p<0.001, Two-tailed Student's t-tests.

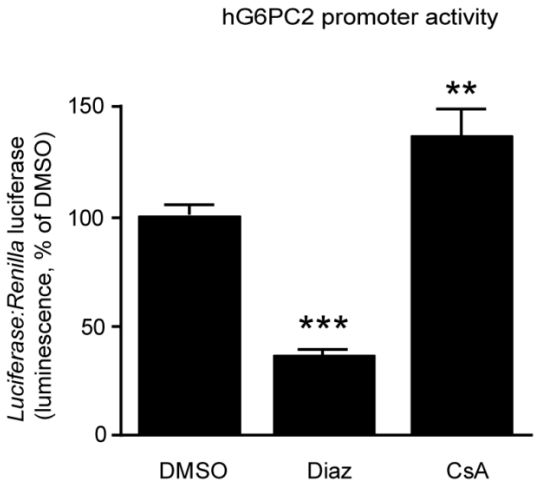

SUPPLEMENTARY DATA

Supplementary Table 1. Oligonucleotide sequences used to design pLKO.1-shSc (scrambled), pLKO.1-shSRI144, and pLKO.1-shSRI457 plasmids.

ShRNA	Direction	Sequence (5' → 3')
Scrambled_ShRNA	Forward	CCGGCCTAAGGTTAAGTCGCCCTCGCTCGAGCGAGGGCGACTTAACCTTAGGTTTTT
	Reverse	AATTCAAAAACCTAAGGTTAAGTCGCCCTCGCTCGAGCGAGGGCGACTTAACCTTAGG
shRNA_SRI144	Forward	CCGGAATTGATGCTGACGAATTGCACTCGAGTGCAATTCGTCAGCATCAATTTTTTTG
	Reverse	AATTCAAAAAAATTGATGCTGACGAATTGCACTCGAGTGCAATTCGTCAGCATCAATT
ShRNA_SRI457	Forward	CCGGAAGATCACGTTTGATGACTACCTCGAGGTAGTCATCAAACGTGATCTTTTTTTG
	Reverse	AATTCAAAAAAAGATCACGTTTGATGACTACCTCGAGGTAGTCATCAAACGTGATCTT

SUPPLEMENTARY DATA

Supplementary Table 2. Characteristics of donor's providing islet samples. Details were provided by the harvesting and processing institution.

Identifier	**Gender**	**Age**	**BMI (kg/m^2)**	**Cause of death**	**Originating facility**
DA1	Male	48	N/A	N/A	Edmonton, Canada
DP2	Female	64	29.4	Cerebral trauma	Pisa, Italy
D03	Female	42	29	N/A	Oxford, United Kingdom
DP4	Female	64	29.4	Cerebral haemorrhage	Pisa, Italy
DP5	Male	78	23.1	Cerebral haemorrhage	Pisa, Italy
DM6	Male	61	33.8	Cerebral bleeding	Milano, Italy
DG7	Female	60	21.5	Cerebral haemorrhage	Geneva, Switzerland
DM8	Male	63	24.5	Cerebral haemorrhage	Milano, Italy
DP9	Male	60	26.1	Cerebral trauma	Pisa, Italy
DM10	Male	64	23.7	Cerebral haemorrhage	Milano, Italy
DM11	Male	47	37.1	Cerebral haemorrhage	Milano, Italy
DA12	N/A	N/A	N/A	N/A	Edmonton, Canada
DM13	Male	52	22.8	Cerebral haemorrhage	Milano, Italy

SUPPLEMENTARY DATA

Supplementary Table 3. Oligonucleotide sequences of primers used for RT-qPCR.

Gene	NCBI No.	Direction	Sequence (5' → 3')
HOMO SAPIENS			
ACTB	NM_001101.3	Forward	TCCCTGGAGAAGAGCTACGA
		Reverse	AGCACTGTGTTGGCGTACAG
CHOP	NM_001195053.1	Forward	TCTTGACCCTGCTTCTCTG
		Reverse	TCTTCCTCCTCTTCCTCCTG
G6PC2	NM_021176.2	Forward	CTGCCCTGAGCCACACTGT
		Reverse	CCAAAAAACACTCCAAAGAAATGAC
GRP78/BIP	NM_005347.4	Forward	TGGCGGAACCTTCGATGT
		Reverse	TGGCCACAACTTCGAAGACA
SRI	NM_003130.3	Forward	GCACCAGCGGGAAGATCA
		Reverse	TGAGAGCCCTCAGTTTGACACA
MUS MUSCULUS			
Actb	NM_007393.3	Forward	TCCCTGGAGAAGAGCTACGA
		Reverse	AGCACTGTGTTGGCGTACAG
Chop	NM_001290183.1	Forward	AGGAGCCAGGGCCAACA
		Reverse	TCTGGAGAGCGAGGGCTTT
G6pc2	NM_021331.4	Forward	CCCATGTCTTGAGCAGTTTCC
		Reverse	ATTGCGTGGCCAGATGGA
GRP78/BIP	NM_001163434.1	Forward	TGGAGTTCCCAGATTGAAG
		Reverse	CCTGACCCACCTTTTTCTCA
Sri	NM_025618	Forward	GCACCAGCGGGAAGATCA
		Reverse	TGAGAGCCCTCAGTTTGACACA
Total Xbp-1	(1)	Forward	TGGCCGGGTCTGCTGAGTCCG
		Reverse	GTCCATGGGAAGATGTTCTGG
Spliced Xbp-1	(1)	Forward	CTGAGTCCGAATCAGGTGCAG
		Reverse	GTCCATGGGAAGATGTTCTGG

(1) from Lipson et al, Cell Metab. 2006 Sep;4(3):245-54.

SUPPLEMENTARY DATA

Supplementary Table 4. Ingenuity Pathway Analysis of microarray dataset. Top ranking networks (score ≥ 30); 1.5 fold-change cut-off, P-value = 0.01.

Probe ID	Score	Focus molecules	Up-regulated (at least 1.5 fold)	Down-regulated (at least 1.5 fold)	Top Diseases and Functions
1	44	25	BBS1, DHCR24*, DYNC1LI1*, KLHL13, NUDCD3*, NUP133*, SAC3D1, VANGL2	ALG5*, ANAPC1*, CCDC64*, CCT3*, CDC6*, CDC45, CDK1*, CENPF, HECW2, KIF1C*, LRRC59*, MAD2L1*, NEDD1*, PDCL3, PRC1, RAD54B*, RRP1B*	Cell Cycle, Cellular Assembly and organization, DNA replication, Recombination and Repair
2	40	23	CLDN4, CNGA3*, DLK1*, ECE1*, ERLIN2*, HS6ST1*, IPRP3, MGAT3, PDE7A, PVRL1*, RGS3*, SRI*, WNK4*	AMPH*, ATP2B4*, CCP110*, CD200*, ITPR1*, JAM2*, PDE5A*, PLCB4, RGS5, SNAP23	Molecular Transport, Cellular Assembly and Organization, Cellular Function and Maintenance
3	34	21	APOF*, HIST2H2AA3/HIST 2H2AA4*, HIST4H4*, INSIG1*, LDLR*, LINGO1, PCOLCE2*, PRKAG3*, RAB3B*, SERPINA1*, SREBF1, ZBTB7C	FABP5*, Gpihbp1*, MKI67, NAP1L1*, PBK, RGCC, SEMA6D*, SLC30A7*, TNFRSF10A*	Lipid Metabolism, Small Molecule Biochemistry, Vitamin and Mineral Metabolism
4	33	20	AMIGO2*, ANXA4*, CISH, DCK, DDR1, IFI16*, IL7R*, JAK3*, KRT75*, MED19*, MED22*, MSH2*, NEUROG3, TLE3*	ALDH7A1, MSH3*, RSL1D1*, SLC2A6, SPPL2A*, TLE3*, TOP2a*	Cellular Development, Haematological System Development and Function, Cancer
5	30	19	ADRBK1*, ANXA11*, AQP7*, ASCL1*, CBLC*, DPYSL2*, FOXO3, GNA13*, GSN*, MAP15*, NOSIP*, OBFC1, SETBP1	CAV1, DOCK4*, KCNIP2, NOSTRIN*, NRCAM*, SDPR	Cancer, Organismal Injury and Abnormalities, Respiratory Disease